



# Effects of different tool microstructures on the precision turning of titanium alloy TC21

Xiaohua Qian<sup>1,2</sup> · Xiongying Duan<sup>1</sup> · Jiyan Zou<sup>1</sup>

Received: 1 October 2019 / Accepted: 27 January 2020 / Published online: 10 February 2020  
© Springer-Verlag London Ltd., part of Springer Nature 2020

## Abstract

Titanium alloys are widely used in the aviation field due to the excellent properties, such as high specific-strength and high-temperature resistance. But the poor machinability of titanium alloys has brought the great difficulty to its machining process. In the cutting process of titanium alloys, tool wear is very serious, and the machining quality is difficult to be guaranteed. As a new type titanium alloy, TC21 alloy has the higher strength and its machinability is less than other titanium alloys. Aiming at the cutting defects in the cutting process of TC21 alloy, three different microstructures, including parallel, perpendicular and wavy grooves, are presented and cut on the rake surface of tools by the laser texturing method. A series of precision turning process of TC21 alloy are implemented on the precision machine using the inserts with different microstructures. The effects of the different microstructures on the chip morphology, turning force, surface morphology, and surface roughness are investigated deeply. The results demonstrate that the tool microstructures have very important role on the turning process of titanium alloys and the wavy microstructure has the best effect in improving the machinability of titanium alloy TC21.

**Keywords** Titanium alloy · Tool microstructure · Precision turning · Chip morphology · Roughness · Cutting force

## 1 Introduction

Titanium alloys have the characteristics of high-strength, small density, high fatigue life, excellent corrosion resistance, and heat resistance, which can greatly reduce structure weight and reduce cost and improve the structure efficiency. So titanium alloy has become one of the most important aviation materials [1–3]. Nevertheless, titanium alloys are very difficult to cut due to low thermal conductivity, strong chemical activity, and low elastic modulus [4–6]. In the machining of titanium alloys, the cutting temperature is high, the tool wear is fast, and the precision is difficult to be ensured, so the poor machinability of titanium alloys limits their application [7–9].

Poor cutting quality is one of the most serious defects in the machining of titanium alloy materials because of the high

chemical activity and low thermal conductivity [10–12]. A lot of research methods have been presented to improve the machinability of titanium alloys [13–23]. Dandekar et al. [13] used the laser-assisted machining to extend the tool life and the material removal rate in the cutting of Ti-6Al-4 V alloy. Lou and Wu [14] adopted the electro-pulsing treatment to change the surface properties for improving the machinability of titanium alloy in ultra-precision cutting. An et al. [15] presented the cold water mist jet cooling method for decreasing cutting temperature in the turning process of titanium alloy TC9. Ganguli and Kapoor [16] investigated the effect of the atomization-based cutting fluid spray equipment in end-milling process of titanium alloy Ti6Al4V. Che-Haron [17] found that the tool life of uncoated cemented carbide tools with finer grain size is longer in the turning process of titanium alloy.

In recent years, many researchers found that the suitable microstructure on the rake surface of tools can improve the machining performance of metal materials [24–31]. Obikawa et al. [24] described the influence of microstructure on the friction conditions on the rake surface in the machining of aluminum alloy. Sugihara and Enomoto [25] proposed various textured surfaces on the cutting tools to extend the tool life in the face milling of steel materials. Enomoto and Sugihara [26]

✉ Xiaohua Qian  
qianxiaohuanit@126.com

<sup>1</sup> Faculty of electronic information and electrical engineering, Dalian university of technology, Dalian 116024, Liaoning Province, China

<sup>2</sup> College of Mechanical and Energy Engineering, Ningbo Institute of Technology, Zhejiang University, Ningbo 315100, China

**Table 1** Mass percentage of various elements of TC21

Ti	Al	Mo	Nb	Sn	Zr	Cr
85.6	5.8	2.4	1.8	2.3	1.9	1.2

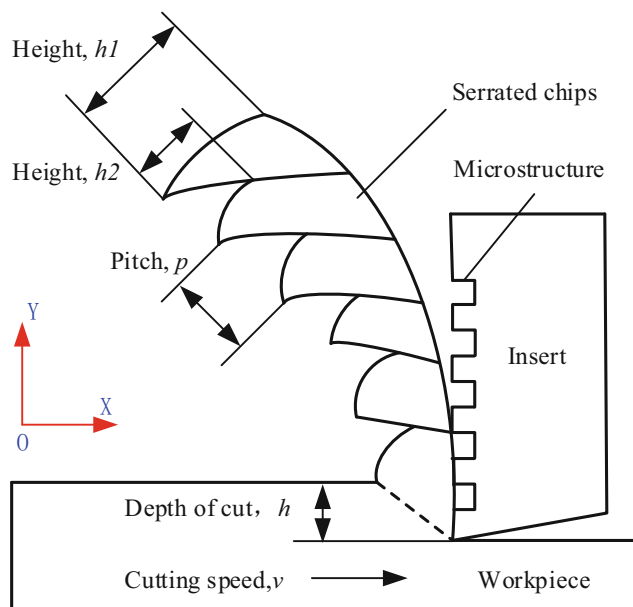
developed the cutting tool with microstructures obtained by the laser machining in the face-milling of aluminum alloy composites. Chang et al. [27] investigated the different microstructures on tool wear in the micro-milling process of NAK80 alloy. Kawasegi et al. [28] developed the new tools with microscale and nanoscale structures on the rake surfaces to control the frictional characteristics of tools in the cutting of aluminum alloy. Koshy and Tovey [29] presented the novel application of electrical discharge machining to generate the isotropic structure on the rake surface of tools for improving the cutting quality.

In addition, many scholars have tried to use the tools with microstructure to cut titanium alloys for improving the machinability [32–35]. Rathod et al. [32] presented the new microstructure tools to improve the cutting quality of titanium alloy. Xie et al. [33] proposed a micro grinding approach to cut micro groove array on rake surface of tools for rapidly dissipating the chips and heat from the shear zone in cutting of titanium alloy without any coolant. Olleak and Özel [34] established 3D finite element model to investigate the influence of microstructure tools on the dry cutting of titanium alloy. Yang et al. [35] investigated the effectiveness of the different micro-grooves on the cutting properties between tool and chip interface in cryogenic minimum quantity lubrication and dry cutting of titanium alloy.

As a new titanium alloy, TC21 alloy has the higher strength and the tool wear in cutting process is more serious than other titanium alloys. At present, the cutting research of this alloy is less. Shi et al. [36] investigated the influence of the cutting parameters, tool wear, and tool material on the milling forces of TC21 alloy in the milling process. Sun et al. [37] analyzed the effectiveness of cutting parameters on cutting temperature, cutting forces, and tool life in the plunge milling of TC21 alloy through a series of experiments. Wu and To [38] established the constitutive material model of TC21 alloy based on the split Hopkinson press bar equipment in high-speed cutting and analyzed the serrated chip formation.

**Table 2** Physical properties of TC21 alloy

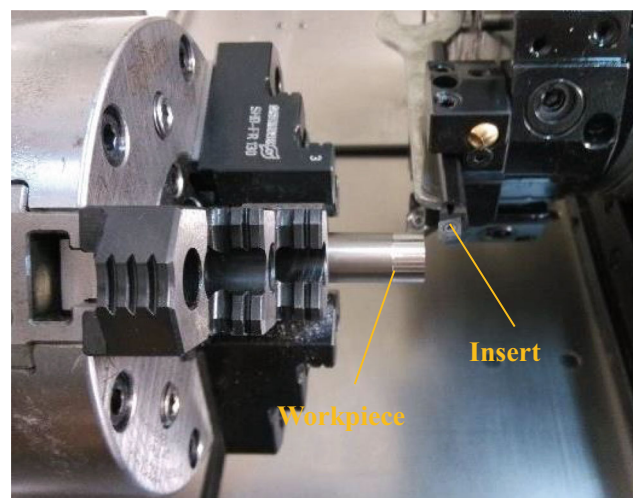
Properties	Value
Hardness (HRC)	42
Density (Kg/m <sup>3</sup> )	4650
Elastic modulus (GPa)	127
Yield strength (MPa)	1190
Melting point (°C)	1755

**Fig. 1** Schematic of the precision turning of titanium alloy

In this paper, in order to reveal the effects of the different microstructures on cutting process of TC21 alloy, three microstructures are cut on the rake surface of tool by the laser machine. A series of precision turning process of TC21 alloy are implemented on the precision lathe machine with these tools. The effects of the microstructures on the chip morphology, turning force, and surface roughness are investigated.

## 2 Experimental setup

In the research, the material of the samples is titanium alloy TC21. The alloy is made of alpha and beta phase and the phase transition temperature is about 950–960 °C. The STEREOSCAN 600 X-ray photoelectron spectroscopy equipment is used to obtain the chemical composition of TC21

**Fig. 2** Experimental setup of precision turning for TC21 alloy

**Table 3** Parameters in the precision turning of TC21 alloy

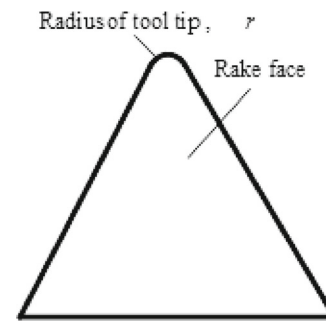
Parameters	Values
Cutting speed, $v$	350 m/min
Feeding speed, $f$	0.0013 mm/rev
Depth of cut, $h$	0.012 mm
Tool material	Carbide without coating
Tool geometric angle,	Rake angle $0^\circ$ , clearance angle $5^\circ$
Radius of tool tip, $r$	0.5 mm
Wavy angle, $a$	$60^\circ$
Step, $s$	$40\ \mu\text{m}$
Height, $h$	$40\ \mu\text{m}$
Cutting environment	Dry cutting

alloy. The dimension of the samples is  $10\ \text{mm} \times 10\ \text{mm} \times 2\ \text{mm}$ , and the measured surface is polished. The measurements are carried out 5 times at the different positions on the sample surface. The mass percentages of the chemical elements are listed in Table 1.

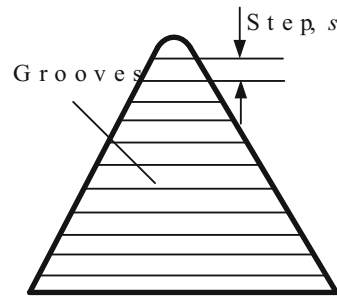
TC21 alloy is one new titanium alloy with high-strength and high toughness. This material can be used in the structural parts of aircraft wing joints, fuselage, and connection frame of landing gear, and important or key load-bearing components requiring high-strength and durability. Its detailed mechanical properties are listed in Table 2.

The schematic of the turning process for TC21 alloy with the tool microstructures is shown in Fig. 1. The practical precision turning experiments of titanium alloys have been performed on a CNC precision machine PD/C-TMC as shown in Fig. 2. The TC21 samples are cylindrical with a diameter of 14 mm and a length of 30 mm in these precision turning experiments. The precision turning parameters of TC21 alloy are listed in Table 3. These parameters are based on the consideration of precision CNC lathe stability and tool durability optimization.

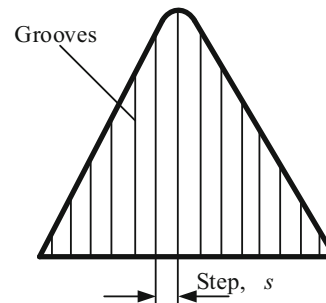
Low thermal conductivity of titanium alloy leads to cutting temperature is higher in the cutting. At high-temperature, the chemical activity of titanium alloy increases greatly and chip is easy to stick to the rake surface. In the turning of titanium alloys, high thermal conductivity, good bending strength, small grain size, and titanium affinity of cemented carbide is often selected as tool material. In this research, the material of inserts is cemented carbide. There are three different microstructures cut on the rake surface of inserts by a 5 axis numerical control laser machine. The power of laser is 200 W, the pulse width is 5 ms and the impulse frequency is 5 Hz. These microstructures are made of many grooves. The schematic of microstructures on the rake face is shown in Fig. 3. And the width and depth of the grooves are both  $20\ \mu\text{m}$ . The other parameters of microstructures are listed in Table 3. The practical images of microstructures on the rake surface are shown in Fig. 4.



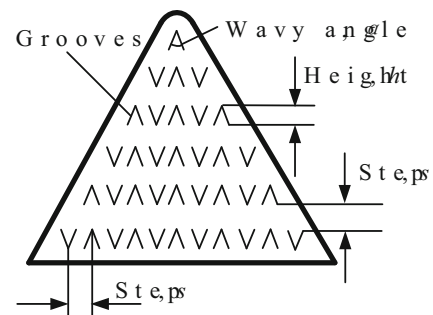
(a) No microstructure



(b) Parallel microstructure

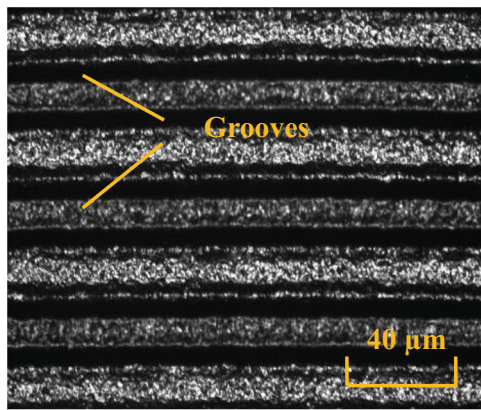


(c) Perpendicular microstructure

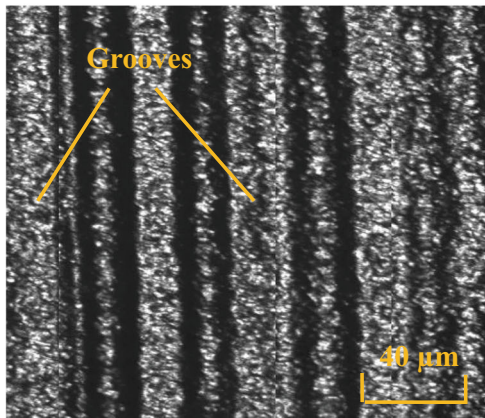


(d) Wavy microstructure

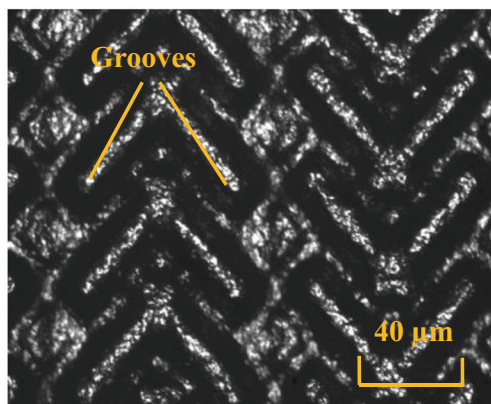
**Fig 3** Schematic of the microstructures on the rake surface of tools for titanium alloy cutting. **a** No microstructure, **b** Parallel microstructure, **c** Perpendicular microstructure, **d** Wavy microstructure



(a) Parallel microstructure



(b) Perpendicular microstructure



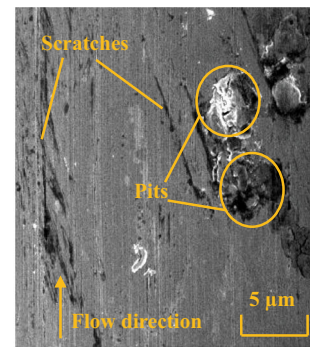
(c) Wavy microstructure

**Fig. 4** Practical microstructures on the rake surface of tools. **a** Parallel microstructure, **b** Perpendicular microstructure, **c** Wavy microstructure

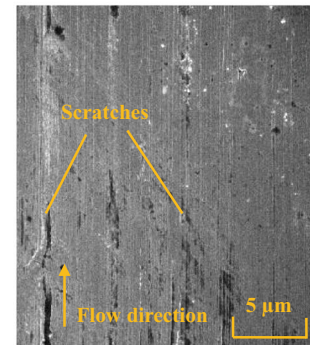
### 3 Results and discussion

#### 3.1 Effect of tool microstructures on the chip morphology

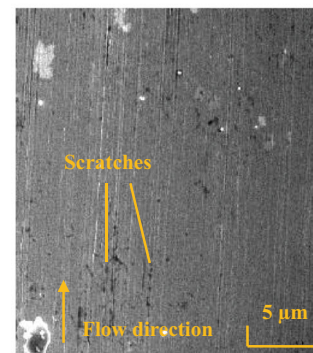
A series of precision turning experiments for titanium alloy TC21 have been carried out. In the cutting tests, four samples



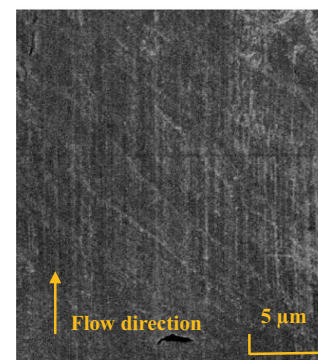
(a) Without microstructure



(b) Horizontal microstructure

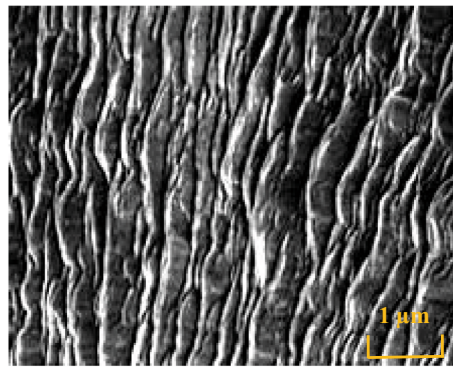


(c) Perpendicular microstructure

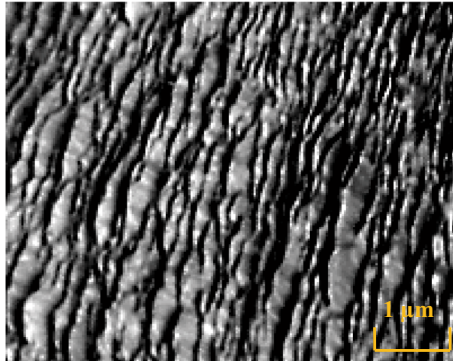


(d) Wavy microstructure

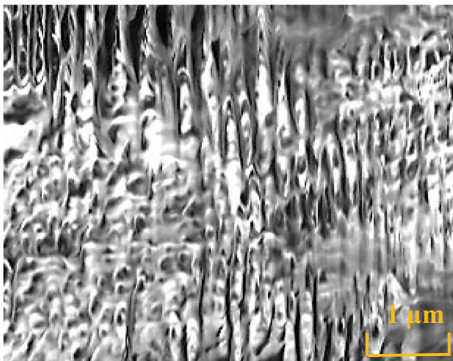
**Fig. 5** Surface morphology of chip contacted with rake surface. **a** Without microstructure, **b** Horizontal microstructure, **c** Perpendicular microstructure, **d** Wavy microstructure



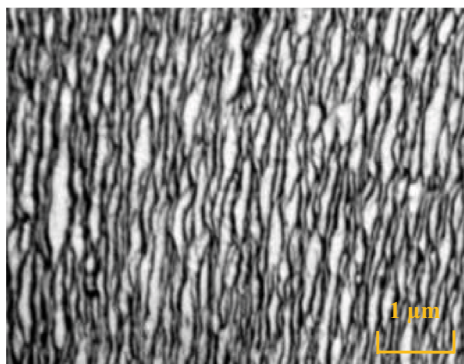
(a) Without microstructure



(b) Parallel microstructure



(c) Perpendicular microstructure



(d) Wavy microstructure

**Fig. 6** Surface morphology of chips under the different tool microstructures. **a** Without microstructure, **b** Parallel microstructure, **c** Perpendicular microstructure, **d** Wavy microstructure

**Table 4** Morphology comparison of serrated chip

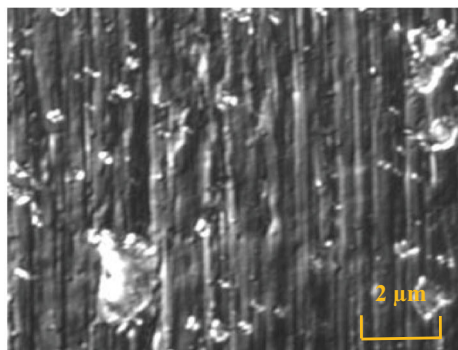
	Pitch, $ph_2/h_1$
Without microstructure	0.45 $\mu\text{m}$ 0.38
Horizontal microstructure	0.33 $\mu\text{m}$ 0.32
Perpendicular microstructure	0.23 $\mu\text{m}$ 0.28
Wavy microstructure	0.19 $\mu\text{m}$ 0.23

and four different inserts are prepared, and each sample is cut 5 times with the same insert, and parameters. The cutting length of each cutting is 20 mm. The surface morphology of chips and the machined surface were measured by the scanning electron microscopy (SEM) after the turning experiments. The SEM images of the chip surfaces contacted with the tool rake surface are shown in Fig. 5. Fig. 5a shows that the chip material is torn into pits and adheres to the rake surface, and there are many scratches on the surface at the same time. While the chip surfaces obtained with three microstructures are smoother than it without microstructure. In addition, although the horizontal and perpendicular microstructure can reduce the defect of chip surface, the surface quality is worse than it with wavy microstructure. Fig. 5d shows that the chip surface is very smooth and the chip flow is very smooth. The results prove that there is little chip material adhering to the rake face and the wavy microstructure can improve the contact between chip and rake face.

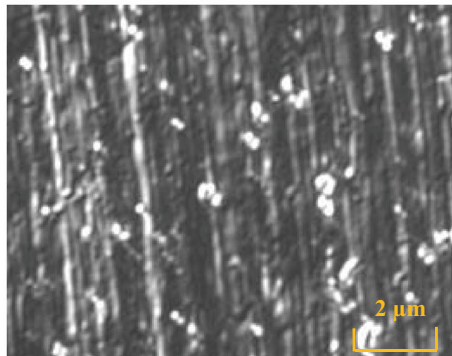
The SEM images of outer chip surface are shown in Fig. 6. The figure shows that the chips are all serrated. It can be seen that the chip surface obtained by the wavy microstructure has the least fluctuation, which will cause less vibration in the cutting force. In Fig. 6a, the serrated pitch is the largest and the degree of serrated is the most significant. While in Fig. 6b, Fig. 6c and Fig. 6d, chips have the lower serration. Among them, the serration of chip is the lowest and chip pitch is the smallest in Fig. 6d. Experimental results confirm that the tool structure changes the chip shape and flow state. This change is due to the change of contact state between the tool rake face and chip. The degree of chip serration can be indicated by  $h_2/h_1$ . And the larger the specific value, the more obvious the serrated. The shape data of the serrated chips are listed in Table 4. It shows that the tool microstructure can reduce the degree of chip serration. And the wavy structure is the most effective, with a 57% reduction in serrated pitch and the 39.5% in the  $h_2/h_1$ .

### 3.2 Effect of tool microstructures on surface morphology and roughness

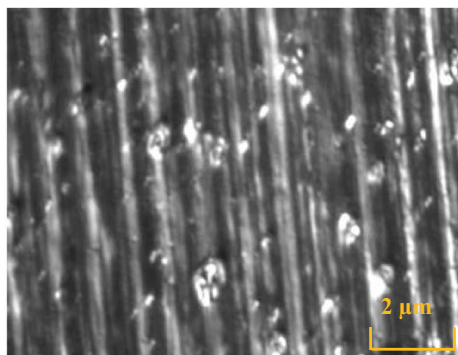
The SEM images of surface morphology of TC21 alloy samples after the precision turning with the different tool microstructures are shown in Fig. 7. It confirms that the surface quality obtained with microstructures is better than without



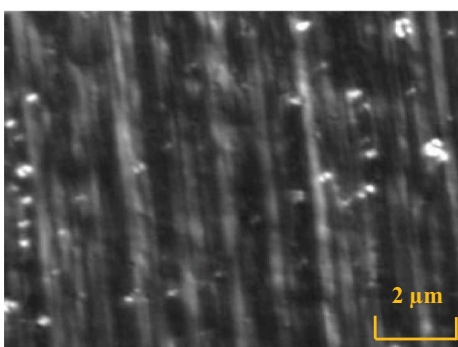
(a) Without microstructure



(b) Parallel microstructure



(c) Perpendicular microstructure



(d) Wavy microstructure

**Fig. 7** Comparison of surface morphology after the precision turning. **a** Without microstructure, **b** Parallel microstructure, **c** Perpendicular microstructure, **d** Wavy microstructure

**Table 5** Comparison of surface roughness

	Mean value of surface roughness, Ra
Without microstructure	0.36 $\mu\text{m}$
Horizontal microstructure	0.31 $\mu\text{m}$
Perpendicular microstructure	0.28 $\mu\text{m}$
Wavy microstructure	0.22 $\mu\text{m}$

microstructure and there are few burrs and defects on the machined surface. And the results demonstrate that the surface quality obtained by the wavy microstructure is the best. This is because the wavy microstructure on the rake face can reduce the adhesion of chip and make chip flow smooth, which will eventually result in smooth material removal, less burrs, and better surface quality.

The surface roughness (Ra) measured by a precision surface roughness measuring device JB-4C after the precision turning experiments. And the measure length is 4 mm. Because five cutting experiments have been carried out with the same cutting parameters for each sample, the mean value of surface roughness is listed in Table 5. The table shows that the surface roughness obtained using the tools with microstructure is better than it without microstructure. The values of Ra with different structures decrease 13.8%, 22.2%, and 38.8%, respectively. The results confirm that the wavy microstructure on the rake face can greatly reduce the value of surface roughness in the precision turning of TC21 alloy.

### 3.3 Effect of tool microstructures on the turning force

The cutting forces in the precision turning experiments of TC21 alloy are obtained by the dynamometers Kistlers 9255B. The primary cutting force curves  $F_x$  under the different microstructures are shown in Fig. 8. It shows that the cutting force vibrated around the average value. The mean value of cutting force is listed in Table 6. It can be seen that the cutting forces with microstructure inserts are smaller than without microstructure insert. The tool microstructure can decrease the cutting force which can be confirmed in the paper [27]. The wavy structure can reduce the cutting force by 18.6%, the vibration amplitude by 45.9%, and the cycle 69.4%. In addition, the cutting force obtained using the wavy microstructure has the least fluctuation and the smallest cycle. And it shows that the degree of serrated chip is minimal with wavy microstructure.

## 4. Conclusions

Poor machinability is one of the primary factors restricting the application of titanium alloys. In this paper, to improve the machinability of titanium alloy TC21 in the cutting process,

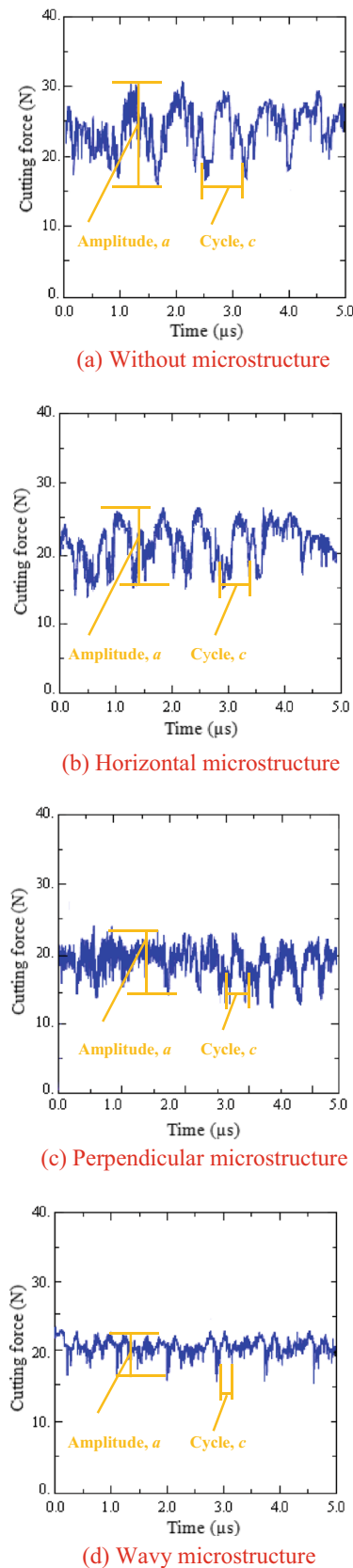


**Fig. 8** Comparison of turning force with different tool microstructures. **a** Without microstructure, **b** Parallel microstructure, **c** Perpendicular microstructure, **d** Wavy microstructure

**Table 6** Comparison of cutting force

	$F_x a c$
Without microstructure	23.6 N 6.1 N 0.85 $\mu$ s
Horizontal microstructure	20.3 N 5.6 N 0.62 $\mu$ s
Perpendicular microstructure	19.7 N 4.9 N 0.43 $\mu$ s
Wavy microstructure	19.2 N 3.3 N 0.26 $\mu$ s

three different microstructures are presented and cut on the rake surface of tools by the laser cutting. A series of precision turning experiments of TC21 alloy have been carried out on the precision lathe machine with these tools. The effects of tool microstructures on chip morphology, turning force, surface morphology, and surface roughness of the machined samples have been investigated. The results show that the tool microstructure has very important role on the turning process of titanium alloy. In addition, the results confirm that the wavy groove has the best effect in the three tool microstructures for the cutting of TC21 alloy. The wavy microstructure can reduce the degree of chip serration, decrease the fluctuation of cutting force and improve the surface quality of TC21 alloy. The advantages of wavy structure are mainly reflected in the following aspects:

- (1) The value of the surface roughness  $R_a$  decreases 38.8%.
- (2) The tool microstructure can reduce effectively the degree of the chip serration, with a 57% reduction in serrated pitch and the 39.5% in the serrated degree of chips.
- (3) The wavy structure can reduce the cutting force by 18.6%, the vibration amplitude by 45.9%, and the cycle 69.4%.

## References

1. Boyer RR, Briggs RD (2005) The use of  $\beta$  titanium alloys in the aerospace industry. *J Mater Eng Perform* 14(6):681–685
2. Brewer WD, Bird RK, Wallace TA (1998) Titanium alloys and processing for high speed aircraft. *MAT SCI ENG A* 243(1–2): 299–304
3. Arrazola PJ, Garay A, Iriarte LM, Armendia M, Marya S, Maître FL (2009) Machinability of titanium alloys (Ti6Al4V and Ti555. 3). *J MATER PROCESS TECH* 209(5):2223–2230
4. Hassan MR, Mershad M, Dawood S (2014) Review of the machining difficulties of nickel-titanium based shape memory alloys. *Appl Mech Mater* 564:533–537
5. Watanabe I, Kiyosue S, Ohkubo C, Aoki T, Okabe T (2002) Machinability of cast commercial titanium alloys. *J Biomed Mater Res* 63(6):760–764
6. Mehrpouya M, Shahedin AM, Dawood SDS, Ariffin AK (2017) An investigation on the optimum machinability of NiTi based shape memory alloy. *Mater Manuf Process* 32(13):1497–1504
7. Rahman M, Wang ZG, Wong YS (2006) A review on high-speed machining of titanium alloys. *JSME INT J C-MECH SY* 49(1):11–20

8. Ezugwu EO, Wang ZM (1997) Titanium alloys and their machinability—a review. *J MATER PROCESS TECH* 68(3):262–274
9. Nabhani F (2001) Machining of aerospace titanium alloys. *ROBOT CIM-INT MANUF* 17(1):99–106
10. Jawaid A, Che-Haron CH, Abdullah A (1999) Tool wear characteristics in turning of titanium alloy Ti-6246. *J MATER PROCESS TECH* 92–93(3):329–334
11. Yang H, Chen Z, Zhou ZT (2015) Influence of cutting speed and tool wear on the surface integrity of the titanium alloy Ti-1023 during milling. *INT J ADV MANUF TECH* 78(5–8):1113–1126
12. Wang ZG, Rahman M, Wong YS (2005) Tool wear characteristics of binderless CBN tools used in high-speed milling of titanium alloys. *WEAR* 258(5):752–758
13. Dandekar CR, Shin YC, Barnes J (2010) Machinability improvement of titanium alloy (Ti–6Al–4V) via LAM and hybrid machining. *Int J Mach Tool Manu* 50(2):174–182
14. Lou YG, Wu HB (2017) Improving machinability of titanium alloy by electro-pulsing treatment in ultra-precision machining. *INT J ADV MANUF TECH* 93(5–8):2299–2304
15. An QL, Fu YC, Xu JH (2011) Experimental study on turning of TC9 titanium alloy with cold water mist jet cooling. *Int J Mach Tool Manu* 51(6):549–555
16. Ganguli S, Kapoor SG (2016) Improving the performance of milling of titanium alloys using the atomization-based cutting fluid application system. *J Manuf Process* 23:29–36
17. Che-Haron CH (2001) Tool life and surface integrity in turning titanium alloy. *J MATER PROCESS TECH* 118(1):231–237
18. Sutter G, List G (2013) Very high speed cutting of Ti–6Al–4V titanium alloy – change in morphology and mechanism of chip formation. *Int J Mach Tool Manu* 66:37–43
19. Glaa N, Mehdi K, Zitoune R (2018) Numerical modeling and experimental analysis of thrust cutting force and torque in drilling process of titanium alloy Ti6Al4V. *INT J ADV MANUF TECH* 96(5–8):2815–2824
20. Wang ZG, Wong YS, Rahman M (2005) High-speed milling of titanium alloys using binderless CBN tools. *Int J Mach Tool Manu* 45(1):105–114
21. Ruibin XB, Wu HB (2016) Study on cutting mechanism of Ti6Al4V in ultra-precision machining. *INT J ADV MANUF TECH* 86(5–8):1311–1317
22. Wu HB, Guo L (2014) Machinability of titanium alloy TC21 under orthogonal turning process. *Mater Manuf Process* 29(11–12):1441–1445
23. Wu HB, Zhang SJ (2015) Effects of cutting conditions on the milling process of titanium alloy Ti6Al4V. *INT J ADV MANUF TECH* 77(9–12):2235–2240
24. Obikawa T, Kamio A, Takaoka H, Osada A (2011) Micro-texture at the coated tool face for high performance cutting. *Int J Mach Tool Manu* 51(12):966–972
25. Sugihara T, Enomoto T (2013) Crater and flank wear resistance of cutting tools having micro textured surfaces. *Precis Eng* 37(4):888–896
26. Enomoto T, Sugihara T (2010) Improving anti-adhesive properties of cutting tool surfaces by nano-/micro-textures. *CIRP ANN-MANUF TECHN* 59(1):597–600
27. Chang W, Sun J, Luo X, Ritchie JM, Mack C (2011) Investigation of microstructured milling tool for deferring tool wear. *WEAR* 271(9):2433–2437
28. Kawasegi N, Sugimori H, Morimoto H, Morita N, Hori I (2009) Development of cutting tools with microscale and nanoscale textures to improve frictional behavior. *Precis Eng* 33(3):248–254
29. Koshy P, Tovey J (2011) Performance of electrical discharge textured cutting tools. *CIRP ANN-MANUF TECHN* 60(1):153–156
30. Dong MK, Lee I, Sun KK, Bo HK, Park HW (2016) Influence of a micropatterned insert on characteristics of the tool–workpiece interface in a hard turning process. *J MATER PROCESS TECH* 229:160–171
31. Li Y, Deng J, Chai Y, Fan W (2016) Surface textures on cemented carbide cutting tools by micro EDM assisted with high-frequency vibration. *INT J ADV MANUF TECH* 82(9–12):2157–2165
32. Rathod P, Aravindan S, Paruchuri VR (2015) Evaluating the effectiveness of the novel surface textured tools in enhancing the machinability of titanium alloy (Ti6Al4V). *J Adv Mech Des Syst* 9(3):1–19
33. Xie J, Luo MJ, He JL, Liu XR, Tan TW (2012) Micro-grinding of micro-groove array on tool rake surface for dry cutting of titanium alloy. *INT J PRECIS ENG MAN* 13(10):1845–1852
34. Olleak A, Özel T (2017) 3D finite element modeling based investigations of micro-textured tool designs in machining titanium alloy Ti-6Al-4V. *Proced Manu* 10:536–545
35. Yang Y, Su Y, Li L, He N, Zhao W (2015) Performance of cemented carbide tools with microgrooves in Ti-6Al-4V titanium alloy cutting. *INT J ADV MANUF TECH* 76(9–12):1731–1738
36. Qi S, Li L, He N, Zhao W, Liu XL (2013) Experimental study in high speed milling of titanium alloy TC21. *INT J ADV MANUF TECH* 64(1–4):49–54
37. Sun T, Fu YC, He L, Chen XM, Zhang WG, Chen W, Su XB (2016) Machinability of plunge milling for damage-tolerant titanium alloy TC21. *INT J ADV MANUF TECH* 85(5–8):1315–1323
38. Wu HB, To S (2015) Serrated chip formation and their adiabatic analysis by using the constitutive model of titanium alloy in high speed cutting. *J ALLOY COMPD* 629:368–373

**Publisher's note** Springer Nature remains neutral with regard to jurisdictional claims in published maps and institutional affiliations.